Playing with the Chaotropic Effect to Improve the Encapsulation of Decaborate Clusters within Cyclodextrins

Zeinab El Hajj, Sergiu Calancea, Mohamed Haouas, David Landy, Daoud Naoufal, Sébastien Floquet

▶ **To cite this version:**

Zeinab El Hajj, Sergiu Calancea, Mohamed Haouas, David Landy, Daoud Naoufal, et al.. Playing with the Chaotropic Effect to Improve the Encapsulation of Decaborate Clusters within Cyclodextrins. Journal of Cluster Science, 2023, 10.1007/s10876-023-02468-x . hal-04180590

HAL Id: hal-04180590
https://hal.science/hal-04180590

Submitted on 12 Aug 2023

HAL is a multi-disciplinary open access archive for the deposit and dissemination of scientific research documents, whether they are published or not. The documents may come from teaching and research institutions in France or abroad, or from public or private research centers.

L'archive ouverte pluridisciplinaire **HAL**, est destinée au dépôt et à la diffusion de documents scientifiques de niveau recherche, publiés ou non, émanant des établissements d'enseignement et de recherche français ou étrangers, des laboratoires publics ou privés.

Playing with the chaotropic effect to improve the encapsulation of decaborate clusters within cyclodextrins.

Zeinab El Hajj,[a,b] Sergiu Calancea,[a] Mohamed Haouas,[a,*] David Landy,[c] Daoud Naoufal,[b] and Sébastien Floquet,[a,*]

a. Institut Lavoisier de Versailles, CNRS, UVSQ, Université Paris-Saclay, 45 av. des Etats-Unis, 78035 Versailles, France

b. Laboratory of Organometallic and coordination chemistry, LCIO, Lebanese University, Faculty of Sciences I, Hadath, Lebanon

c. Unité de Chimie Environnementale et Interactions sur le Vivants (UCEIV, EA 4492), ULCO, Dunkerque, France

* Corresponding authors. e-mail : mohamed.haouas@uvsq.fr, sebastien.floquet@uvsq.fr

Abstract: This paper deals with the formation of host-guest systems between α, β and γ cyclodextrins and the anionic cluster $[B_{10}H_9NCCH_3]^-$. The inclusion processes within cyclodextrins were evidenced in solution by ESI-MS and NMR, while ITC measurements provided thermodynamic parameters and affinity constants with cyclodextrin. These studies confirm the chaotropic character of this anion and evidence inclusion processes much more favored than that found for the dianionic $[B_{10}H_{10}]^{2-}$ cluster previously reported. This result evidences that playing on the volume and the charge of chaotropic systems can dramatically improve the encapsulation process within cyclodextrins.

Keywords : decaborate • cyclodextrin • chaotrope • host-guest chemistry

Introduction

Boranes represent a wide family of clusters of interest not only for fundamental research but also in many different domains such as energetic materials[1–3], catalysis[4,5], extraction of radioactive wastes[6] or in medicine[7–9]. For example, boron clusters are chemical agents for Boron Neutron Capture Therapy (BNCT) used for cancer treatment[1,8,9].

Particularly motivated by their biological properties, great attention is given to the study of carboranes, derivatives of the $[B_{12}H_{12}]^{2-}$ and the $[B_{10}H_{10}]^{2-}$ cluster. The latter offers the possibility of various selective functionalizations[10,11]. For instance, the *closo*-decaborate-triethoxysilane is used as precursor for grafting to luminescent dye doped silica nanoparticles, thus facilitating the tracing of the *closo*-decaborate drug pathway in BNCT[12,13]. Similarly, the *closo*-decaborate cluster has been successfully covalently attached to polyoxometalate compounds, well known for their electron storage properties that are very useful in many fields, including biology.[14,15]

Cyclodextrins (CDs) are natural macrocyclic oligosaccharides comprised of 6, 7 and 8 D-glucopyranose units, named as α-, β- and γ-CD, respectively. Because of their robustness, non-toxicity, and ability to host a wide variety of organic or inorganic guest species in aqueous media[16–21], CDs are attractive for the design of drug delivery systems. Among the many host-guest systems, several boranes, carboranes or metallocarboranes inclusion compounds formed with cyclodextrins are reported in the literature following different strategies[22–29]. In particular, Nau, Gabel, Assaf, and coworkers reported very interesting works focused on the inclusion compounds formed with dodecaborate derivatives[30–34]. They demonstrated the formation of very stable host-guest complexes with clusters of the type $[B_{12}X_{12}]^{2-}$ and $[B_{12}X_{11}Y]^{2-}$ (X = H, Cl, Br, I and Y = OH, SH, NH_3^+, NR_3^+, a dye or a fulorescein), which is rationalized by a chaotropic effect as driving force of the supramolecular assembly. Chaotropic or super-chaotropic anions decrease the water structure in their direct solvation shell. Their inclusion within the cavity of CDs provokes the release of these high-energy water solvates to the bulk. Such a water structure recovery is governed by a negative entropy variation and an enthalpic process. The super-chaotropic nature of dodecaborate derivatives has been nicely described[33], and we also evidenced that the *closo*-decahydrodecaborate cluster $[B_{10}H_{10}]^{2-}$ is slightly chaotropic[35].

The charge density is one of the most important parameters. It can be tuned to modify the inclusion process as demonstrated on dodecaborate clusters, polyoxometalates, and metallic

clusters M_6X_n[17–19]. Therefore, to increase the chaotropic character of $[B_{10}H_{10}]^{2-}$ and thus enhance the affinity for its encapsulation in CDs, one can plan to play with its volume and charge.

In this study, we selected the cluster $[B_{10}H_9NCCH_3]^-$,[36] which is a bit bigger than $[B_{10}H_{10}]^{2-}$ and less charged (see Figure 1). Moreover, the addition of a substituent on the B_{10} cluster should also contribute to break the symmetry around the cluster and avoid the organization of water solvates, a key point for the chaotropic effect. For such a cluster, the encapsulation process must be favored compared to that of $[B_{10}H_{10}]^{2-}$. Herein, the encapsulation of $[B_{10}H_9NCCH_3]^-$ within α-, β- and γ-CD, will systematically be studied by ESI-MS, NMR and ITC.

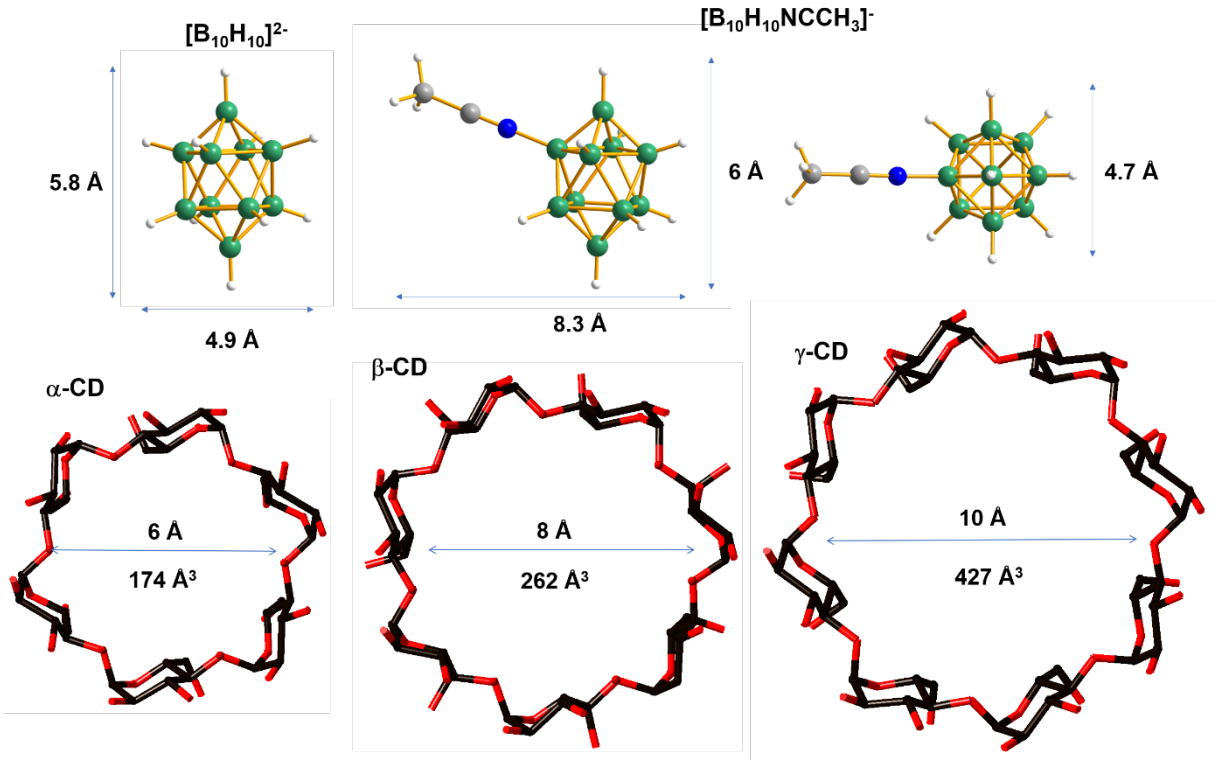

Figure 1. Molecular structures of the clusters $[B_{10}H_{10}]^{2-}$ and $[B_{10}H_{10}NCCH_3]^-$ with α–, β–, and γ-cyclodextrins highlighting host and guest sizes.

Experimental section

Physical methods

Fourier Transform Infrared (FT-IR) spectra were recorded on a 6700 FT-IR Nicolet spectrophotometer, using diamond ATR technique. ATR correction was applied. **Elemental**

analyses of C, H, and N were carried out by the analytical service of the CNRS at Gif sur Yvette, France.

Electrospray Ionization Mass Spectrometry (ESI-MS) spectra were collected using a Q-TOF instrument supplied by WATERS. Samples were solubilized in water at a concentration of 10^{-4} M and were introduced into the spectrometer via an ACQUITY UPLC WATERS system whilst a Leucine Enkephalin solution was co-injected via a micro pump as internal standard.

Nuclear magnetic resonance (NMR) solution spectra were recorded at 25 °C in D_2O. ^{1}H and ^{11}B NMR were measured with a Bruker Avance 400 MHz spectrometer equipped with a 5 mm BBI probe head and operated at a magnetic field strength of 9.4 T. Quartz NMR tubes are used to avoid background signals from standard glass tubes in case of ^{11}B. Typically, ^{1}H spectra were recorded with one pulse sequence at 30° flip angle (pulse duration 2.4 μs), using 1 s recycle delay, 1.6 s acquisition time, and 80 number of scans. In case of samples containing boron, ^{11}B decoupling was systematically applied during the acquisition of ^{1}H spectra. The ^{11}B spectra were recorded with Hahn echo sequence (echo delay 117 μs) under proton decoupling condition, using 0.1 s recycle delay, 21 ms acquisition time, and 1024 number of scans. Chemical shifts are reported relative to 1% Me_4Si in $CDCl_3$ for ^{1}H, and 15% $BF_3.Et_2O$ in $CDCl_3$ for ^{11}B using external standards[37].

Isothermal titration calorimetry ITC. Formation constants and inclusion enthalpies of host-guest systems $[B_{10}H_{10}NCCH_3]^-$@CD were simultaneously determined for each system by the use of an isothermal calorimeter (ITC200, MicroCal Inc.), at 298 K. Degassed water solutions were used in both cell (202.8 μL) and syringe (40 μL).

Each $(Et_3NH)[B_{10}H_{10}NCCH_3]$ system was studied by titration (injection of 5 mM CD solution on a 0.5 mM $(Et_3NH)[B_{10}H_{10}NCCH_3]$ solution) and release (injection of 5 mM CD and 5 mM $(Et_3NH)[B_{10}H_{10}NCCH_3]$ solution on water solution) protocols. Experiments involved one initial aliquot of 0.5 μL followed by ten aliquots of 3.5 μL of the syringe solution, delivered over 7 s for each injection. Time interval between two consecutive injections and agitation speed were set to 90 s and 1000 rpm, respectively.

The resulting heat flow was recorded as a function of time. The heat of dilution was eliminated from each titration by subtracting the raw signal obtained for the corresponding blank titrations. The peak area following each addition was obtained by integration of the resulting signal and was expressed as the heat effect per injection. Thermodynamic parameters were determined by

global nonlinear regression analysis of the titration and release isotherms, using a dedicated homemade program[38].

Syntheses

All reagents were purchased from commercial sources and used without further purification. $(Et_3NH)_2[B_{10}H_{10}]$ is provided by katchem company.

Synthesis of $(Et_3NH)[B_{10}H_{10}NCCH_3]$

The synthesis of $(Et_3NH)[B_{10}H_{10}NCCH_3]$ was performed according to literature procedure[36] from $(Et_3NH)_2[B_{10}H_{10}]$ and characterized by ESI-MS, FT-IR, and NMR. FT-IR/cm^{-1} (ATR Diamond): 3075 (s), 2510 (s, BH), 2467 (s, CN), 1476 (m), 1461 (m), 1451 (m), 1404 (m), 1389 (m), 1364 (m), 1299 (w), 1156 (m), 1072 (w), 1033 (w), 1001 (s), 936 (w), 881 (w), 835 (m), 813 (w), 777 (w). $^1H\{^{11}B\}$ NMR (δ ppm, CD_3CN) : 0.10 (1H), 0.30 (2H), 0.36 (2H), 0.80 (2H), 2.46 (3H, Me), 3.29 (1H), 3.36 (1H), 1.29 (9H, Et_3NH^+), 3.21 (6H, Et_3NH^+), 6.70 (3H, Et_3NH^+) ; $^{11}B\{^1H\}$ NMR (δ ppm, CD_3CN) : 3.36 (1B), -2.3 (1B), -20.9 (1B), -26.1 (2B), -26.8 (2B), -28.7 (3B). ESI-MS (CH_3CN) *m/z* found 176.19 (calculated for $\{[B_{10}H_{10}NCCH_3](H_2O)\}^-$ *m/z* 176.25).

Results and discussion

Syntheses

The synthesis of $(Et_3NH)[B_{10}H_{10}NCCH_3]$ was performed according to literature procedure[36] by reaction of acetonitrile with $[B_{10}H_{10}]^{2-}$ in presence of trifluoroacetic acid. $(Et_3NH)[B_{10}H_{10}NCCH_3]$ was isolated as colorless crystals and used without further purification. FT-IR, ESI-MS and NMR spectra are in perfect agreement with the expected compound. Note that the ^{11}B and ^1H NMR spectra recorded in CD_3CN need decoupling from ^1H and ^{11}B nuclei respectively to facilitate the assignments of all signals and to be sure that there is no unreacted compound $(Et_3NH)_2[B_{10}H_{10}]$ as shown in Figures 2 and 3. In particular, the ^1H spectrum without decoupling from ^{11}B leads to broad multiplets that it is difficult to assign confidently (Figure 3b).

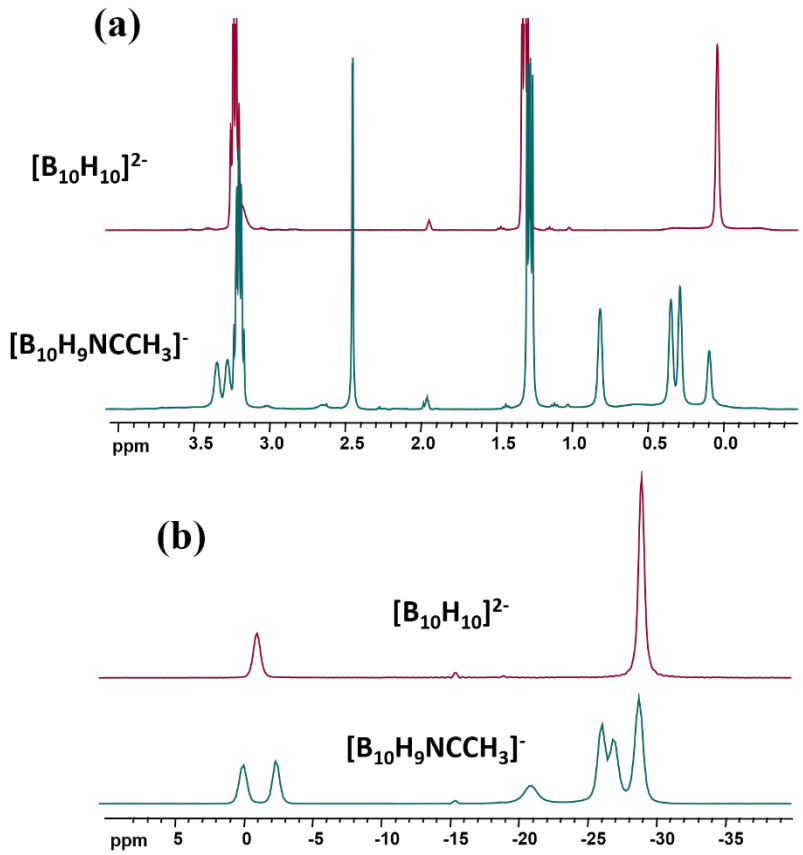

Figure 2. $^{1}H\{^{11}B\}$ NMR spectra (a) and $^{11}B\{^{1}H\}$ NMR spectra (b) in CD_3CN of $(Et_3NH)[B_{10}H_9NCCH_3]$ in comparison with $(Et_3NH)_2[B_{10}H_{10}]$.

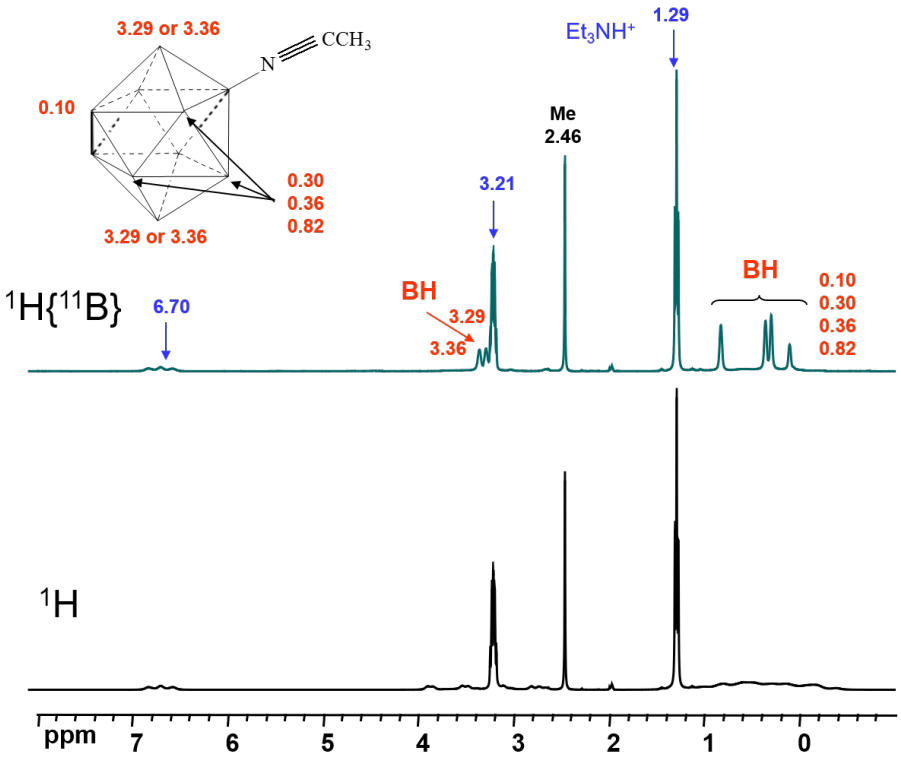

Figure 3. ^{1}H and $^{1}H\{^{11}B\}$ NMR spectra of $(Et_3NH)[B_{10}H_9NCCH_3]$ in CD_3CN with the attributions of signals.

ESI-MS

Following our previous work concerning $[B_{10}H_{10}]^{2-}$ encapsulation within CD[35], we decided to analyse 10^{-5} M aqueous mixtures of $(Et_3NH)[B_{10}H_9NCCH_3]$ and α–, β-, or γ-CD with 1:1 ratios. The ESI-MS spectra are given in Figure 4. All spectra show the same peak at *m/z* 176.19 which can be assigned to the monoanionic species $\{B_{10}H_9NCCH_3(H_2O)\}^-$. The free CD appears as a monoanionc species $\{(CD)\text{-}H\}^-$ at *m/z* 971.31 (α-CD), 1134.37 (β-CD) and 1296.43 (γ-CD). The formation of 1:1 adducts as dianionic species, $\{(B_{10}H_9NCCH_3)(CD)(H_2O)\text{-}H\}^{2-}$, is confirmed by the peaks at *m/z* 547.25, 655.28 and 736.30 for α-, β- and γ-CD, respectively. The relative low intensity peaks of free α-CD and its 1:1 adduct compared to those of β-CD and γ-CD suggests the lower boron cluster affinity for the α-CD and probably a less efficient encapsulation.

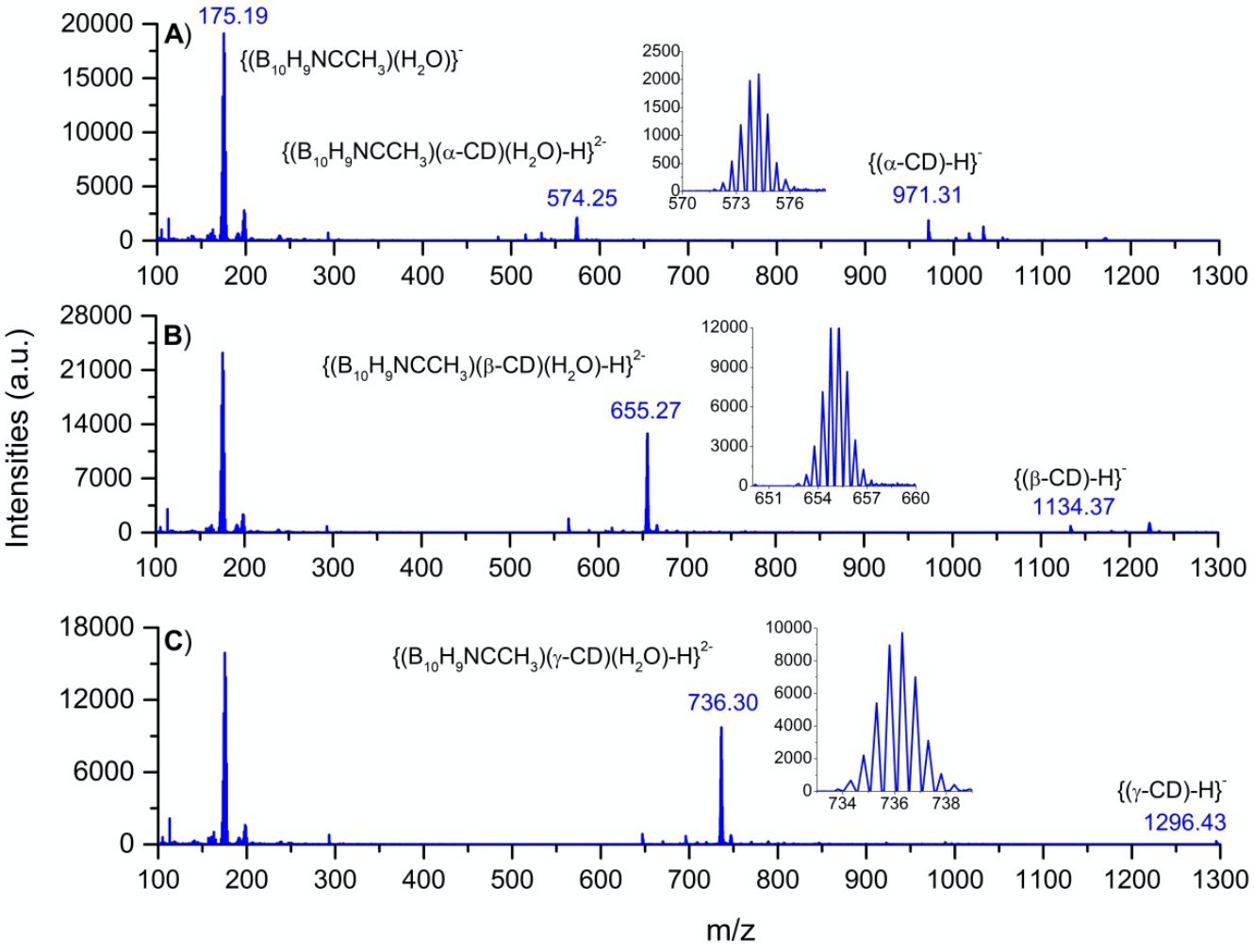

Figure 4. ESI-MS spectra of the aqueous mixtures in 1:1 ratio of $(Et_3NH)[B_{10}H_9NCCH_3]$ (10^{-5} M) and α-CD **(a)**, β-CD **(b)** and γ-CD **(c)**.

NMR study of the interaction between cyclodextrins and $(Et_3NH)_2[B_{10}H_9NCCH_3]$ in D_2O.

In a previous paper, we studied the encapsulation process of the cluster $[B_{10}H_{10}]^{2-}$ by using its ammonium salt. In the present case, the triethylammonium salt of $[B_{10}H_9NCCH_3]^-$ was used. In order to verify that the counter cation cannot play a significant role in the encapsulation process, a titration of β-CD by Et_3NHCl was first realized. By adding up to 8 equivalents of Et_3NHCl per CD, no significant change of the NMR spectrum of the CD was seen. This counter-cation plays no competitive role in CD complexation and the observed effects are solely due to the interaction of the boron cluster with the host.

The encapsulation of $(Et_3NH)[B_{10}H_9NCCH_3]$ cluster within the cavity of α-, β or γ-CD have been monitored by ^1H NMR titration of 3 mM aqueous CD solutions with $B_{10}H_9NCCH_3^-$. The ^1H spectra of various $[B_{10}H_9NCCH_3]^-$/CD mixtures are depicted in Figures 5-7.

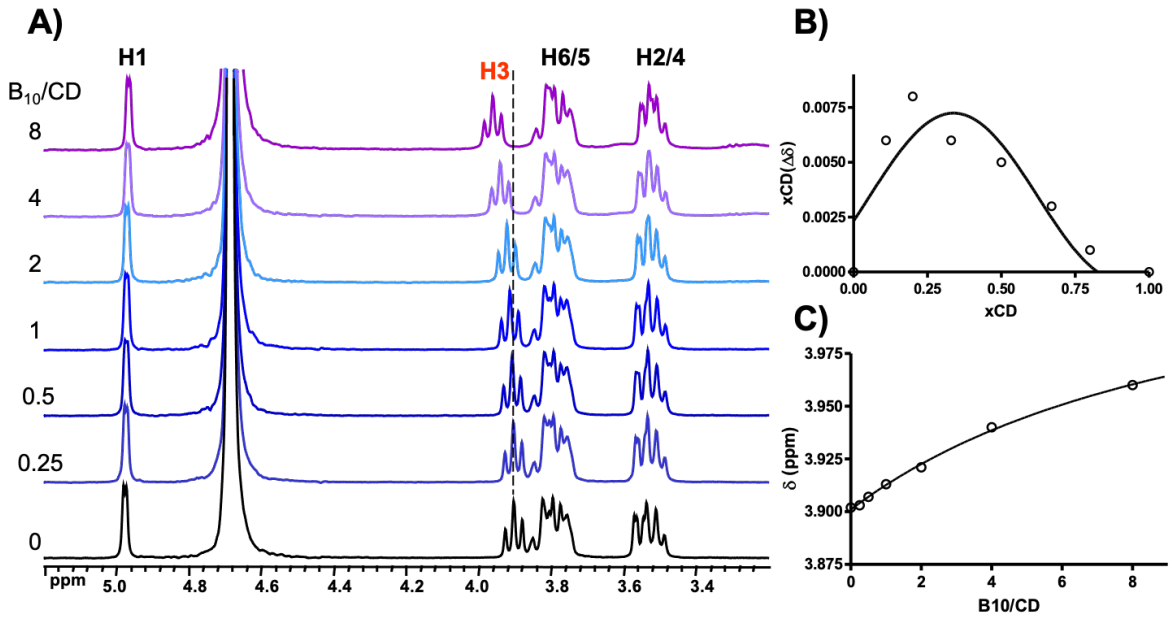

Figure 5. ^1H NMR spectra in D_2O for different ratios of $B_{10}H_9NCCH_3^-$/α-CD from the titration of 3 mM aqueous α-CD solution with $B_{10}H_9NCCH_3^-$ **(A)**, *Job's plot* - the product of molar fraction in CD (xCD) and chemical shift variations of H3 internal protons ($\Delta\delta = \delta_{obs} - \delta_{H3}$) versus xCD, the molar fraction of CD within the mixture **(B),** and observed chemical shift varitions of α-CD-H3 internal protons versus $B_{10}H_9NCCH_3^-$ content **(C)**.

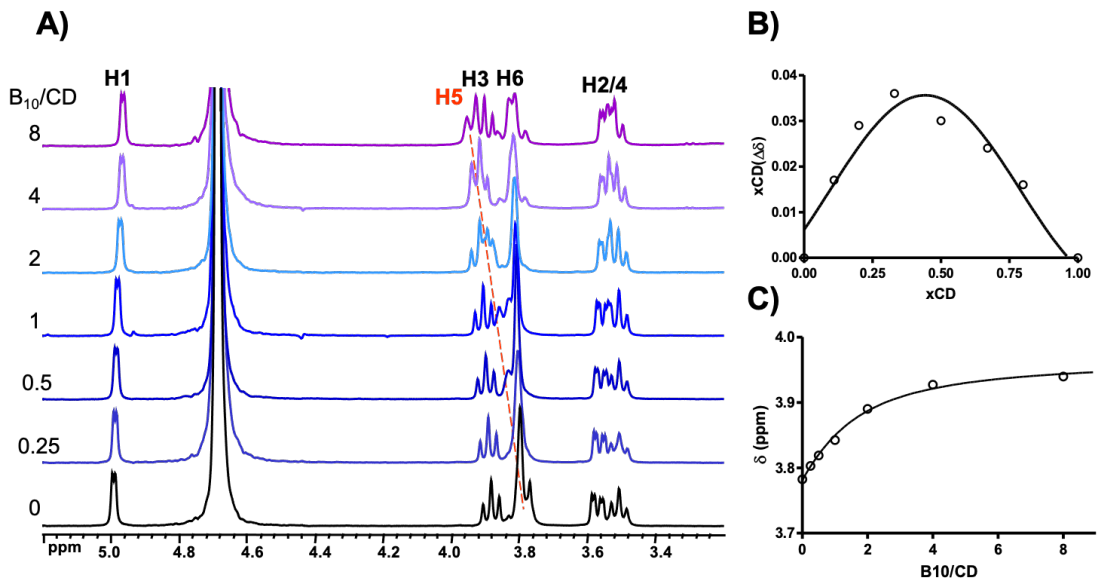

Figure 6. ^{1}H NMR spectra in D_2O for different ratios of $B_{10}H_9NCCH_3^-$/β-CD from the titration of 3 mM aqueous β-CD solution with $B_{10}H_9NCCH_3^-$ **(A)**, *Job's plot* - the product of molar fraction in CD (xCD) and chemical shift variations of H5 internal protons ($\Delta\delta = \delta_{obs} - \delta_{H5}$) versus xCD **(B),** and observed chemical shift varitions of β-CD-H5 internal protons versus $B_{10}H_9NCCH_3^-$ content (**C**).

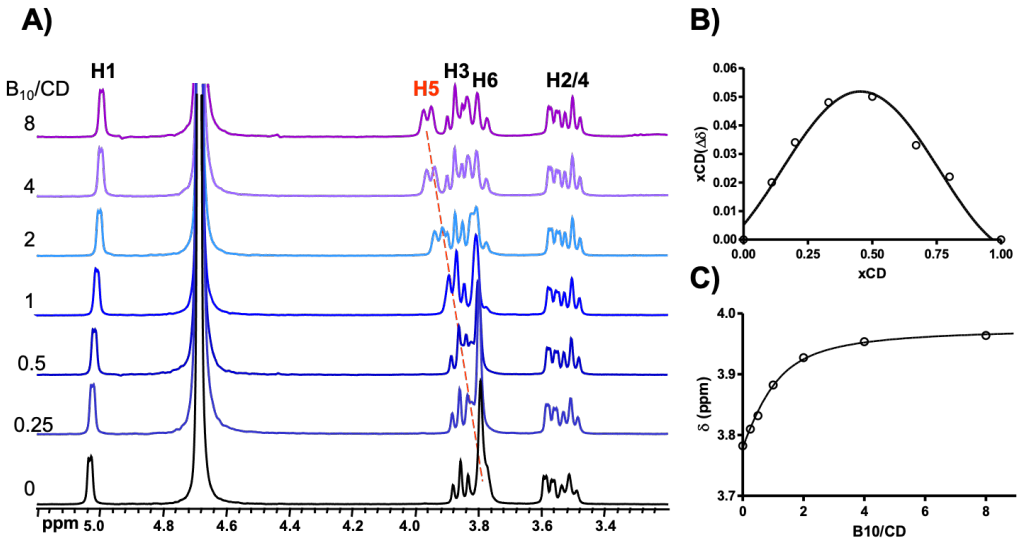

Figure 7. ^{1}H NMR spectra in D_2O for different ratios of $B_{10}H_9NCCH_3^-$/γ-CD from the titration of 3 mM aqueous γ-CD solution with $B_{10}H_9NCCH_3^-$ **(A)**, *Job's plot* - the product of molar fraction in CD (xCD) and chemical shift variations of H5 internal protons ($\Delta\delta = \delta_{obs} - \delta_{H5}$) versus xCD **(B),** and observed chemical shift varitions of γ-CD-H5 internal protons versus $B_{10}H_9NCCH_3^-$ content (**C**).

As reported in our previous studies[35], the boron cluster encapsulation into CDs can induce slight shifts variation of the internal protons corresponding to the primary (H5 and H6) and/or secondary (H3) CDs faces (see Scheme 1).

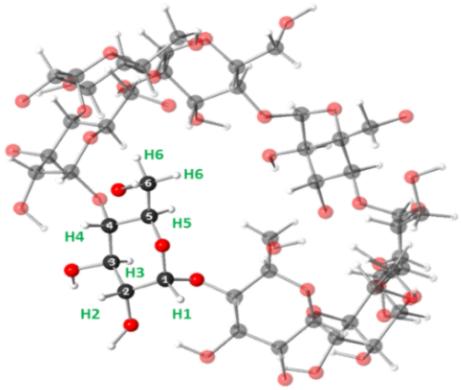

Scheme 1. Numbering of protons within a cyclodextrin.

Thus, in the case of α-CD (Figure 5A) the increasing of $[B_{10}H_9NCCH_3]^-$/α-CD ratio induces no major changes in the NMR spectra except of a slight shift of H3 protons with a maximum variation of only +0.058 ppm (Figure 5C). This demonstrates weak interactions of the CD with the cluster. Titration of β– and γ-CD with $[B_{10}H_9NCCH_3]^-$ cluster (Figures 6A and 7A) is however leading to a stronger shift of H5-CDs protons. The maximum variation is up to +0.157 and +0.182 ppm for $[B_{10}H_9NCCH_3]^-$/β-CD and $[B_{10}H_9NCCH_3]^-$/γ-CD mixtures, respectively (Figures 6C and 7C). This behaviour suggests stronger interactions of boron cluster with β-CD and γ-CDs.

The Job's plots (Figures 5B-7B), which represent the product of the molar fraction in CD (*x* CD) and chemical shift variations of H3 or H5 protons ($\Delta\delta = \delta_{obs}-\delta_{H3\text{ or }H5}$) versus *x* CD, under boron cluster titration allow to determine the adducts stoichiometry. In the case of β-CD and γ-CD (Figures 6B and 7B), the curves clearly show a maximum at *x* CD about 0.5, consistent with the formation of 1:1 adducts, $\{(B_{10}H_9NCCH_3)(CD)\}$. Concerning α-CD, the variation of chemical shift of H3 is very small and the Job's plot (Figure 5B) does not permit to see a clear maximum on the curve. It suggests a weaker interactions of the boron cluster with α-CD on its outer surface in a random fashion and the observed variation in the chemical shift of H3 does not reflect the formation of a two components adduct.

Finally, the association constants of boron cluster to CDs have been determined from NMR titration applying mathematical approach[39]. As the NMR spectra indicate a fast chemical exchange regime, the observed chemical shift variations of H3 or H5 protons (δ_{obs}) of CD should correspond to a linear combination of the chemical shifts of the free CD and the 1:1

adduct (equation 1), noted δ_0 and $\delta_{1:1}$ respectively. The x_0 and $x_{1:1}$ are the CD molar fractions in free state and in 1:1 adduct correspondingly.

$$\delta_{obs} = x_0\delta_0 + x_{1:1}\delta_{1:1} \qquad (eq.\ 1)$$

Considering a 1:1 adduct, the association constant K is given by equation 2, using the CD molar fractions x_0 and $x_{1:1}$ and expressed as a function of the initial concentration of CD C^0 and the molar ratio $R = [B_{10}H_9NCCH_3]/[CD]$.

$$K = \frac{x_{1:1}}{x_0\left(R - \left(\frac{1 - x_0 + x_{1:1}}{2}\right)\right)C^0} \qquad (eq.\ 2)$$

By combining equations 1 and 2, and considering that $x_0 + x_{1:1} = 1$, one can deduce the expression of the observed chemical shift as a function of binding constant K (equation 3).

$$\delta_{obs} = \delta_0\left[\frac{KC^0 - KC^0R - 1 + \sqrt{(KC^0R - KC^0 + 1)^2 + 4KC^0}}{2KC^0}\right] + \delta_{1:1}\left[\frac{KC^0 + KC^0R + 1 - \sqrt{(KC^0R - KC^0 + 1)^2 + 4KC^0}}{2KC^0}\right]$$

(eq. 3)

Modeling the experimental data leads to the binding constants gathered in Table 1. The best fits of the variation of the experimental chemical shift δ_{obs} as a function of the ratio $R = B_{10}/CD$ according to the equation 3 using these *K* values are shown in Figures 5C, 6C and 7C. The simulated variation of δ_{obs} matches well the experimental data.

Table 1. Formation constant *K* (M^{-1}) of the 1:1 adduct complexes formed between $(Et_3NH)[B_{10}H_9NCCH_3]$ and native cyclodextrins (α-CD, β-CD and γ-CD), obtained from ^1H chemical shifts at 298 K (equation 3) in comparison with formation constants obtained by ITC (vide infra) and previous data[35] obtained with $[B_{10}H_{10}]^{2-}$.

		NMR	ITC
$(Et_3NH)[B_{10}H_9NCCH_3]$	α-CD	34.1 ± 0.8	45 ± 11
	β-CD	300 ± 20	149 ± 4
	γ-CD	720 ± 40	577 ± 8
$(NH_4)_2[B_{10}H_{10}]$[35]	α-CD	35 ± 10	4 ± 3
	β-CD	110 ± 70	40 ± 4
	γ-CD	60 ± 20	19 ± 5

The association constants found by NMR first evidence that *K* values increase in the following order α-CD < β-CD < γ-CD, suggesting again the low affinity of boron cluster to the α-CD and an optimal affinity with the γ-CD. Previously, the optimal affinity of $[B_{10}H_{10}]^{2-}$ was found for β-CD, while the cavity of γ-CD was too large to accommodate this cluster[35]. In the present case, the volume of the cluster $[B_{10}H_9NCCH_3]^-$ is a little higher and logically the γ-CD is better adapted. Secondly, these data, in agreement with ITC data (vide infra) evidence that the affinity constants are improved for host-guest systems with β-CD and γ-CD by replacing $[B_{10}H_{10}]^{2-}$ by $[B_{10}H_9NCCH_3]^-$. The affinity constant for γ-CD appears 12 times higher with $[B_{10}H_9NCCH_3]^-$, as expected due to the chaotropic effect. Finally, for both clusters, the affinity for α-CD appears very weak as the size of the cavity of the host also play a crucial role.

Association constants and thermodynamic data by ITC.

Even if association constants of labile host-guest complexes in aqueous solution can be determined from NMR titrations, isothermal calorimetric titration (ITC) measurements usually lead to more reliable data. In a previous study, we demonstrated the encapsulation of $[B_{10}H_{10}]^{2-}$ was characterized by weak interactions between the host and the guest. In such a case, dedicated protocols have been employed for ITC measurements, *i.e.* release, annihilated release and reverse titration experiments, in order to increase the accuracy of ITC characterization[35]. In the case of $[B_{10}H_9NCCH_3]^-$, the affinity constant appears one order of magnitude higher. Therefore, the $(Et_3NH)[B_{10}H_{10}NCCH_3]$@CD systems were studied by titration (injection of 5 mM CD solution on a 0.5 mM $(Et_3NH)[B_{10}H_{10}NCCH_3]$ solution) and release (injection of 5 mM CD and 5 mM $(Et_3NH)[B_{10}H_{10}NCCH_3]$ solution on water solution) protocols and thermodynamic parameters were determined by global nonlinear regression analysis of these experiments[38]. The corresponding ITC thermograms and isotherms are given in Figure 8, while the thermodynamic parameters are gathered in Table 2.

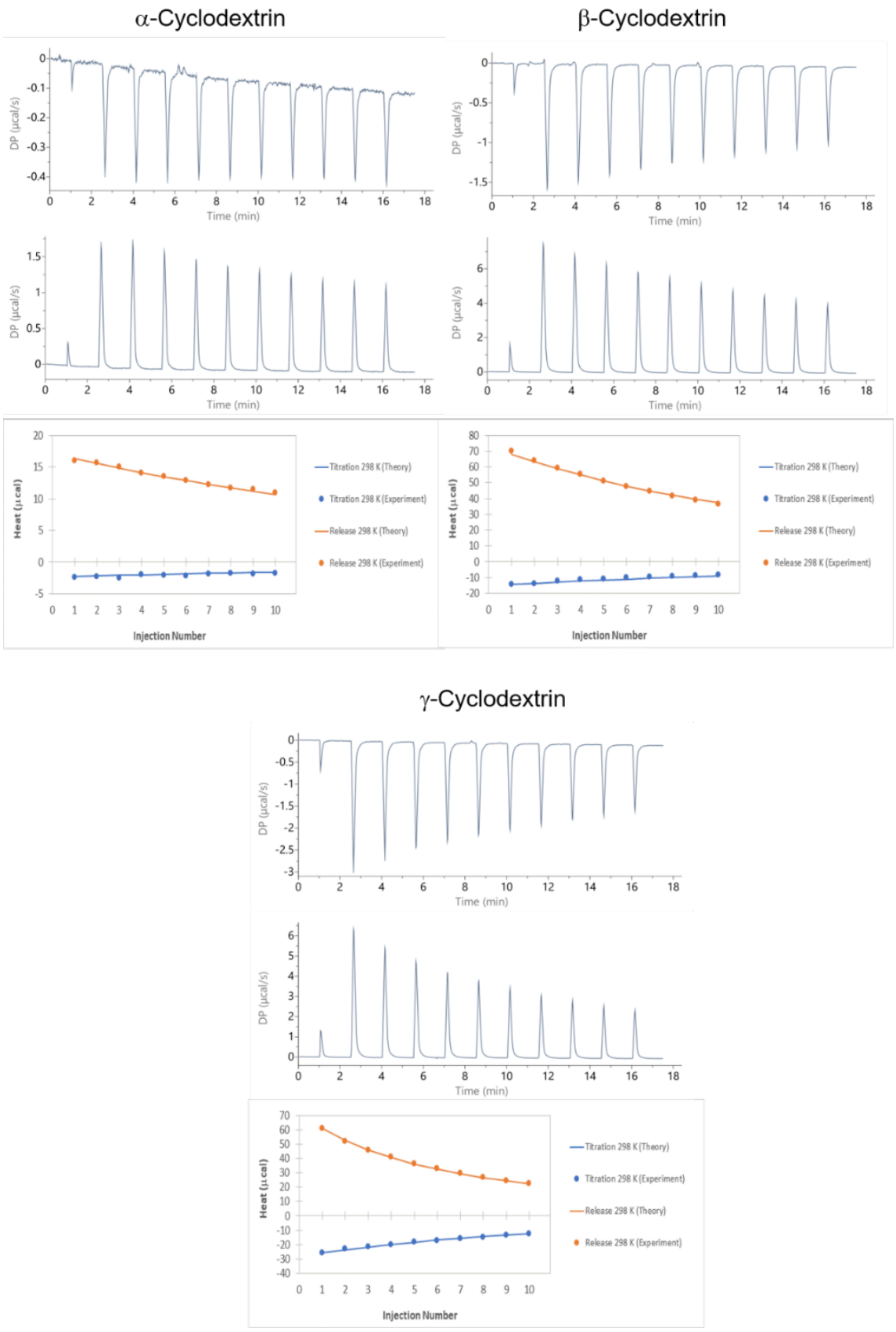

Figure 8: ITC thermograms obtained respectively for the titration and release experiments at 298 K (upper part) and global analysis of experimental isotherms (lower part) for the systems $[B_{10}H_9NCCH_3]^-$/CD (α, β and γ). Dots and lines correspond to experimental and theoretical heats, respectively.

Table 2. Binding constants, enthalpy, entropy and free energy of 1:1 adduct complexes formation between $(Et_3NH)[B_{10}H_9NCCH_3]$ or $(NH_4)_2[B_{10}H_{10}]$[35] and native cyclodextrins (α-CD, β-CD and γ-CD), obtained from ITC data, at 298 K.

		K (M^{-1})	ΔH ($kJ.mol^{-1}$)	TΔS ($kJ.mol^{-1}$)	ΔG ($kJ.mol^{-1}$)
$(Et_3NH)[B_{10}H_9NCCH_3]$	α-CD	45 ± 11	-25.2 ± 4.1	-15.8 ± 4.7	-9.4 ± 0.6
	β-CD	149 ± 4	-51.2 ± 0.5	-39.2 ± 0.6	-12.4 ± 0.1
	γ-CD	577 ± 8	-29.1 ± 0.1	-13.4 ± 0.2	-15.7 ± 0.1
$(NH_4)_2[B_{10}H_{10}]$[35]	α-CD	4 ± 3	-25 ± 16	-21 ± 16	-2.9 ± 1.6
	β-CD	40 ± 4	-34.7 ± 0.8	-25.5 ± 1.2	-9.2 ± 0.5
	γ-CD	19 ± 5	-39.7 ± 2.0	-32.2 ± 2.8	-7.5 ± 0.9

All experimental data agree with a 1:1 stoichiometric model. As expected from a qualitative evaluation of the ITC isotherms, inclusion of $[B_{10}H_9NCCH_3]^-$ in α-CD, β-CD and γ-CD were characterized by an important compensation between a strong enthalpic stabilization and a slightly lower entropic destabilization, leading to significant affinities: 45, 149 and 577 M^{-1} for α-CD, β-CD and γ-CD, respectively, in agreement with NMR studies.

From a thermodynamic point of view, the negative enthalpy values found in all cases demonstrate the process of encapsulation of the $[B_{10}H_9NCCH_3]^-$ cluster is enthalpically driven while the negative entropy variations indicate that the inclusion process of the monoanionic $[B_{10}H_9NCCH_3]^-$ within cyclodextrins is associated to a chaotropic effect, in agreement with our previous study on $[B_{10}H_{10}]^{2-}$ and the works of Nau and coworkers[30,32,34] for dodecaborane derivatives $[B_{12}X_{12}]^{2-}$. This solvent effect can be explained by the migration of the borate cluster from the bulk aqueous medium into the pockets of CD allowing the recovery of the water structure distorted by the chaotropes.

The strength of the chaotropic behavior is notably related to the volume charge density of the anion. Lower chaotropic effect is expected when the volume charge density increases[33,40]. From $[B_{10}H_{10}]^{2-}$ to $[B_{10}H_9NCCH_3]^-$, the volume charge density decreases and thus the chaotropic character of the latter is increased, resulting in an increase in the entropy change associated with the recovery of the water structure upon inclusion in CDs.

Additionally, as commonly observed for cyclodextrins, the increasing of enthalpic contribution is counterbalanced by an increasing entropy penalty which is called enthalpy-entropy compensation. Figure 9 gives the ΔH *vs* TΔS plot associated to the 1:1 complexes of $[B_{10}H_9NCCH_3]^-$, with CDs (red dots) in comparison to previous thermodynamic data[35] reported for $[B_{10}H_{10}]^{2-}$ and for dodecaborate derivatives. The thermodynamic parameters determined for adducts obtained with $[B_{10}H_9NCCH_3]^-$ showed a stronger enthalpy-entropy compensation contrast which is the typical signature of the chaotropic effect in the complexation of CDs[32].

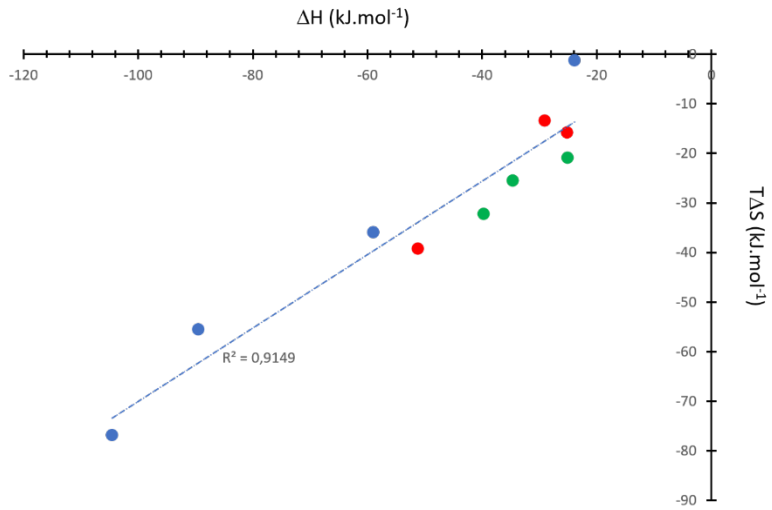

Figure 9: Enthalpy-entropy compensation plot for 1:1 complexes formed between between α-CD, β-CD and γ-CD with $[B_{10}H_{10}]^{2-}$ (green dots)[35], $[B_{10}H_{10}NCCH_3]^-$ (red dots) and $[B_{12}X_{12}]^{2-}$ derivatives (blue dots).

Conclusion

This work reports the host-guest process involving the anionic cluster $[B_{10}H_9NCCH_3]^-$, with α-, β- and γ-cyclodextrins. Solution studies performed by ESI-MS, NMR and ITC with the three CDs allowed demonstrating the formation of 1:1 inclusion complexes between $[B_{10}H_9NCCH_3]^-$ and CDs for which the association constants were determined by NMR and ITC. Both techniques evidence a drastic enhancement of the encapsulation process of $[B_{10}H_9NCCH_3]^-$ compared to $[B_{10}H_{10}]^{2-}$, while the most stable host-guest system is obtained with γ-CD.

The ITC studies evidences the chaotropic character of the cluster $[B_{10}H_9NCCH_3]^-$. The increase of stability compared to previous studies with $[B_{10}H_{10}]^{2-}$, perfectly matches with a higher chaotropic effect expected when the charge density decreases. The less charged and more voluminous $[B_{10}H_9NCCH_3]^-$, induces a change in its solvation properties that favors adsorption

onto hydrophobic cavities such as the macrocyclic CDs. Nevertheless, this effect of solvent alone on the encapsulation process of $[B_{10}H_9NCCH_3]^-$ could not be sufficient and the size-matching effect between host and guest may also play an important role.

Nevertheless, this process remains moderate. In fact, even if the global charge is 1-, locally the charge of the "$B_{10}H_9$" moiety globally remains of 2- while a 1+ charge is localized on the nitrogen atom of the grafted acetonitrile molecule. A stronger effect would be probably observed if the delocalization of the charge occurs on the entire molecule. This work is now in progress.

Acknowledgements

We acknowledge the Centre National de la Recherche Scientifique (CNRS) and the Ministère de l'Education Nationale de l'Enseignement Supérieur, de la Recherche et de l'Innovation (MESRI) for their financial support. CampusFrance is gratefully acknowledged for its support through an Excellence Eiffel doctoral grant for ZH and by a mobility program PHC CEDRE (project POMBORON n°42237UG). This work was supported by a public grant overseen by the French National Research Agency as part of the ''Investissements d'Avenir'' program (Labex Charm3at, ANR-11-LABX-0039-grant).

References

[1] B. Hansen, M. Paskevicius, H. Li, E. Akiba, T. Jensen, *Coord. Chem. Rev.* **2016**, *323*, 60–70.
[2] I. Sivaev, *Chem. Heterocycl. Compd.* **2017**, *53*, 638–658.
[3] Y. Zhu, S. Gao, N. Hosmane, *Inorganica Chim. Acta* **2018**, *471*, 577–586.
[4] Y. Zhu, N. Hosmane, *J. Organomet. Chem.* **2013**, *747*, 25–29.
[5] Y. Zhu, N. Hosmane, *Coord. Chem. Rev.* **2015**, *293*, 357–367.
[6] D. Naoufal, B. Gruner, P. Selucky, B. Bonnetot, H. Mongeot, *J. Radioanal. Nucl. Chem.* **2005**, *266*, 145–148.
[7] I. Sivaev, V. Bregadze, N. Kuznetsov, *Russ. Chem. Bull.* **2002**, *51*, 1362–1374.
[8] Y. Zhu, N. Hosmane, *PURE Appl. Chem.* **2018**, *90*, 653–663.
[9] Y. Zhu, N. Hosmane, *Future Med. Chem.* **2013**, *5*, 705–714.
[10] N. Mahfouz, F. Ghaida, Z. El Hajj, M. Diab, S. Floquet, A. Mehdi, D. Naoufal, *Chem. Sel.* **2022**, *7*, DOI 10.1002/slct.202200770.
[11] I. B. Sivaev, A. V. Prikaznov, D. Naoufal, *Collect. Czechoslov. Chem. Commun.* **2010**, *75*, 1149–1199.
[12] F. Abi-Ghaida, S. Clement, A. Safa, D. Naoufal, A. Mehdi, *J. Nanomater.* **2015**, *2015*, 608432.

[13] F. Abi-Ghaida, Z. Laila, G. Ibrahim, D. Naoufal, A. Mehdi, *Dalton Trans.* **2014**, *43*, 13087–13095.
[14] M. Diab, A. Mateo, J. Al Cheikh, M. Haouas, A. Ranjbari, F. Bourdreux, D. Naoufal, E. Cadot, C. Bo, S. Floquet, *Dalton Trans.* **2020**, *49*, 4685–4689.
[15] M. Diab, A. Mateo, J. El Cheikh, Z. El Hajj, M. Haouas, A. Ranjbari, V. Guerineau, D. Touboul, N. Leclerc, E. Cadot, D. Naoufal, C. Bo, S. Floquet, *Molecules* **2022**, *27*, DOI 10.3390/molecules27227663.
[16] P. A. Abramov, A. A. Ivanov, M. A. Shestopalov, M. A. Moussawi, E. Cadot, S. Floquet, M. Haouas, M. N. Sokolov, *J. Clust. Sci.* **2018**, *29*, 9–13.
[17] A. Ivanov, C. Falaise, P. Abramov, M. Shestopalov, K. Kirakci, K. Lang, M. Moussawi, M. Sokolov, N. Naumov, S. Floquet, D. Landy, M. Haouas, K. Brylev, Y. Mironov, Y. Molard, S. Cordier, E. Cadot, *Chem.- Eur. J.* **2018**, *24*, 13467–13478.
[18] A. A. Ivanov, C. Falaise, D. Landy, M. Haouas, Y. Mironov, M. A. Shestopalov, E. Cadot, *Chem. Commun.* **2019**, *55*, 9951–9954.
[19] S. Khlifi, J. Marrot, M. Haouas, W. Shepard, C. Falaise, E. Cadot, *J. Am. Chem. Soc.* **2022**, *144*, 4469–4477.
[20] M. A. Moussawi, N. Leclerc-Laronze, S. Floquet, P. A. Abramov, M. N. Sokolov, S. Cordier, A. Ponchel, E. Monflier, H. Bricout, D. Landy, M. Haouas, J. Marrot, E. Cadot, *J. Am. Chem. Soc.* **2017**, *139*, 12793–12803.
[21] G. Izzet, M. Ménand, B. Matt, S. Renaudineau, L.-M. Chamoreau, M. Sollogoub, A. Proust, *Angew. Chem. Int. Ed.* **2012**, *51*, 487–490.
[22] J. Warneke, C. Jenne, J. Bernarding, V. Azov, M. Plaumann, *Chem. Commun.* **2016**, *52*, 6300–6303.
[23] P. Neirynck, J. Schimer, P. Jonkheijm, L. Milroy, P. Cigler, L. Brunsveld, *J. Mater. Chem. B* **2015**, *3*, 539–545.
[24] H. Ching, D. Buck, M. Bhadbhade, J. Collins, L. Rendina, *Chem. Commun.* **2012**, *48*, 880–882.
[25] M. Uchman, P. Jurkiewicz, P. Cigler, B. Gruner, M. Hof, K. Prochazka, P. Matejicek, *Langmuir* **2010**, *26*, 6268–6275.
[26] C. Frixa, M. Scobie, S. Black, A. Thompson, M. Threadgill, *Chem. Commun.* **2002**, 2876–2877.
[27] K. Ohta, S. Konno, Y. Endo, *Chem. Pharm. Bull. (Tokyo)* **2009**, *57*, 307–310.
[28] S. Eyrilmez, E. Bernhardt, J. Davalos, M. Lepsik, P. Hobza, K. Assaf, W. Nau, J. Holub, J. Oliva-Enrich, J. Fanfrlik, D. Hnyk, *Phys. Chem. Chem. Phys.* **2017**, *19*, 11748–11752.
[29] J. Nekvinda, B. Gruner, D. Gabel, W. Nau, K. Assaf, *Chem.- Eur. J.* **2018**, *24*, 12970–12975.
[30] K. Assaf, O. Suckova, N. Al Danaf, V. von Glasenapp, D. Gabel, W. Nau, *Org. Lett.* **2016**, *18*, 932–935.
[31] K. Assaf, D. Gabel, W. Zimmermann, W. Nau, *Org. Biomol. Chem.* **2016**, *14*, 7702–7706.
[32] K. I. Assaf, M. S. Ural, F. Pan, T. Georgiev, S. Simova, K. Rissanen, D. Gabel, W. M. Nau, *Angew. Chem. Int. Ed.* **2015**, *54*, 6852–6856.
[33] K. I. Assaf, W. M. Nau, *Angew. Chem. Int. Ed.* **2018**, *57*, 13968–13981.
[34] J. Zhang, D. Gabel, K. Assaf, W. Nau, *Org. Lett.* **2022**, *24*, 9184–9188.
[35] M. Diab, S. Floquet, M. Haouas, P. A. Abramov, X. Lopez, D. Landy, A. Damond, C. Falaise, V. Guerineau, D. Touboul, D. Naoufal, E. Cadot, *Eur. J. Inorg. Chem.* **2019**, *2019*, 3373–3382.
[36] D. Dou, I. Mavunkal, J. Bauer, C. Knobler, M. Hawthorne, S. Shore, *Inorg. Chem.* **1994**, *33*, 6432–6434.

[37] R. Harris, E. Becker, S. De Menezes, R. Goodfellow, P. Granger, *PURE Appl. Chem.* **2001**, *73*, 1795–1818.
[38] E. Bertaut, D. Landy, *Beilstein J. Org. Chem.* **2014**, *10*, 2630–2641.
[39] S. Yao, C. Falaise, S. Khlifi, N. Leclerc, M. Haouas, D. Landy, E. Cadot, *Inorg. Chem.* **2021**, *60*, 7433–7441.
[40] T. Buchecker, P. Schmid, S. Renaudineau, O. Diat, A. Proust, A. Pfitzner, P. Bauduin, *Chem. Commun.* **2018**, *54*, 1833–1836.